Desalination and Water Treatment
www.deswater.com

doi: 10.1080/19443994.2015.1111806

57 (2016) 20307–20317
September

Taylor & Francis
Taylor & Francis Group

Implementation of radial basic function networks for the prediction of RO membrane performances by using a complex transport model

Farshid Iranmanesh[a], Ali Moradi[b,*], Mehdi Rafizadeh[c]

[a]*Chemical Engineering Department, Shahid Bahonar University of Kerman, P.O. Box 76175-133, Kerman, Iran, email: farshidiranmanesh@yahoo.com*
[b]*Petrochemical Department, Iran Polymer and Petrochemical Institute, P.O. Box 115/14965, Tehran, Iran, Tel. +98 9121879563; emails: moradia@mail.uk.ac.ir, moradi@mail.uk.ac.ir, alimoradi2006@yahoo.com*
[c]*Polymer & Color Engineering Department, Amir Kabir University of Technology, Tehran, Iran, Tel. +98 2164542405; email: mehdi@aut.ac.ir*

Received 6 December 2013; Accepted 8 October 2015

ABSTRACT

The main purpose of this research was the prediction of reverse osmosis (RO) membranes performances, including separation factor, pure solvent flux, and total flux. The modified surface force-pore flow is a mathematical and mechanism base model that has predicated the performances of RO membranes appropriately better than others. The equations of this model are complex and nonlinear, which should be solved by an advanced numerical method eventually. In this research, the radial basic function (RBF) network, which is an exclusive typical of artificial neural network (ANN) and an association of radial functions into a single hidden layer, was implemented for the predication of RO membrane performances. The input data of the network were the parameters of this mathematical model and some experimental data which had been obtained from four different types of RO membranes. About 80% of the total experimental data were implemented for the training of data-set and the remaining 20% were used for the testing of data-set. The predictive ability of RBF network was evaluated correctly by the mean square error, root mean square error, and correlation coefficient (R). The mean square errors for training and for testing data-set consequently were obtained 0.00009 and 0.00016 (for separation factor), 0.00013 and 0.00013 (for pure solvent flux), and 0.00009 and 0.00012 (for total flux), respectively. The results showed that this technique has predicted the performances of RO membrane more correctly vs. the experimental data comparing to the previous ANNs and comparing to original model, that is, modified surface force pore flow model accordingly.

Keywords: Artificial neural network; MD-SF-PF model; Radial basic function; RO membrane; Performances; Radial basic function

1. Introduction

Potable and soft water is largely produced by the use of reverse osmosis (RO) membrane processes currently. RO and nanofiltration (NF) are usually implemented for a wide range of applications. They may be classified as solvent purification and solute concentration, in which permeate is desired product and/or concentrated feed is desired product. In this

*Corresponding author.

way, RO mainly uses the membrane types that are permeable to water but essentially impermeable to salt [1–3].

To describe the performances of RO membranes, mathematical and mechanistic models are being used extensively. Some of these models rely on simple concepts such as irreversible thermodynamic models that are nonmechanism base models [4–8]. The other models, especially porous mechanism-based models, are more complex and require sophisticated solution techniques. Therefore, the prediction of RO membrane performances were enhanced by transport models which have been developed over time [9–14].

Among the offered models, the surface force-pore flow (SF-PF) model, which were presented by Sourirajan and Matsuura [15,16], and its modified one (MD-SF-PF), which was later formulated by Mehdizadeh and Dickson, have delivered truthful results [17,18].

Although the MD-SF-PF model is an efficient model for the prediction of RO membrane performances, it involves many interrelated equations, and moreover, some of them are fairly complex and nonlinear, which requires an advanced numerical technique for solving them [19]. Therefore, other techniques, such as artificial neural networks, (ANNs) which do not need the solving of such complex equations, are more valuable for simulating these kinds of models.

During past two decades, applications of neural networks (NNs) have been developed in various fields such as chemistry and environmental studies. ANNs are well-organized predictive methods in the modeling of nonlinear dynamic systems such as membrane processes. One of the primary advantages of ANNs over theoretical approaches is that they consider as black box models, which does not require any complicated governing with forceful assumption equations. Neural networks introduced by McCulloch and Pitts which is based on the interconnection of neurons in the brain [20]. Recently, applications of NNs for the modeling of membrane processes have been developed due to their attractive feature consequently. Niemi et al. used the neural network model for obtaining an estimation of permeable flux and rejection through membrane, and then, their results were compared with those obtained by conventional methods [21,22]. Abbas and Al-Bastaki used a feedforward neural network to predict the performance of a RO experimental setup, which used a Film Tech SW30 membrane [23]. In that research, the Levenberg–Marquardton (LM) was employed for the training of NN. Zoubi et al. used ANNs and Spiegler–Kedem model for the modeling of three commercial NF membranes (NF90, NF270, and N30F) and for different salts (KCl, Na_2SO_4, and $MgSO_4$) at high concentrations similar to those of seawater [24]. These kinds of models that rely on irreversible thermodynamics are nonmechanism-based models and have not high accurate results. Zhao et al. developed two ANNs models by solution diffusion (SD) model and modified SD-based model (hybrid model) to compare actual and predicted permeable stream TDS [25]. One ANN model was used multilayer perceptron (MLP) and the other ANN model used a normal radial basic function (RBF). These membrane models due to their simplicity have high usage but do not have desirable results. Shetty and Chellam employed a back-propagation feedforward network with three layers, (one input, one output, and one hidden) to predict the long-term fouling NF membranes that are used to purify contaminated water supplies [26]. Recently, Lee et al. used a feedforward neural network with three layers to predict the performance of a seawater reverse osmosis desalination plan [27]. The input layer contains five neurons (time, feed temperature, feed concentration, pressure difference ΔP, and feed flow rate), an output layer with two neurons (permeate TDS, and permeate flow rate), and one hidden layer with 15 neurons. Libotean et al. performed a neural network with back-propagation and support vector regression algorithm for a RO plan performance to describe temporal variations in permeate flux and salt passage with a unique capability for useful short-time forecasting of process performance degradation [28]. A new study by Khayet et al. have been done and a MLP feedforward ANN model with four inputs, two hidden layer, and one output layer was used for the prediction of performance index of RO pilot plant [29]. The input factors are feed concentration, feed pressure, feed temperature, and feed flow rate and the outputs is performance index (average between permeable flux and the salt rejection). Jafar and Zilouchian used a radial basis function network (RBFN) to model the performances of two RO plants with different feed water intakes [30]. Chen and Kim developed a RBF neural network (RBFNN) to predict long-term permeate flux decline in crossover membrane filtration [31]. Noghabi et al. used ANN to predict the permeate flux and rejection of ionic compounds of sugar beet press water through polyamide NF membrane [32].

Considering the high capability of MD-SF-PF model and its conditional input data and parameters and available experimental data relevant to the physical conditions of some kinds of membranes, the predication of RO membrane performances via ANN technique by use of these data could conclude some novel and valuable results [17,18]. For the first time, Moradi et al. trained a back-propagation feedforward

neural network to predict the performances of RO membranes process by applying the parameters of MD-SF-PF model [33]. For this study, the Levenberg–Marquardton was selected as training algorithm and the network consists of three layers, including nine neurons in input layer, one neuron in output layer, and 20 neurons in hidden layer. Levenberg–Marquardton is a kind of backpropagation neural network (BPNN), but the RBFNN technique can overcome some of the limitations of BPNN by use of a rapid training phase due having a simple architecture and maintaining complicated mapping abilities.

The main objective of the present work is to develop a RBFNN technique to predict membrane performances based on the parameters of MD-SF-PF model. In this way, the separation characteristics mainly separation factor, pure solvent flux, and total flux will be calculated based on the parameters of MD-SF-PF model and membrane properties such as pore radius, friction constants between solute and solvent and membrane, respectively, and finally operational conditions such as the average longitude concentration of solute in membrane, pressure, and temperature. It can be expected that RBFNN could predict these objective performances with acceptable error. Based on our knowledge, this is the first research which used RBFNN for the prediction of RO membrane performances based on MD-SF-PF model.

2. Theory

2.1. RO performances

The RO membrane performances are introduced as pure solvent (N_p) and total flux (N_t) and separation factor (f). They can be influenced by several factors such as pressure, temperature, concentration of feed water etc. [14,15]. Pure solvent and total flux are defined as the rate of mass transfer of pure solvent per membrane surface and total mass transfer per membrane surface.

Separation factor is defined as the difference between concentrations of feed water near the membrane and permeate water as is shown in Fig. 1 and presented in Eq. (1):

$$f = \frac{C_{A2} - C_{A3}}{C_{A1}} \tag{1}$$

2.2. MD-SF-PF model

The surface force-pore model (SF-PF) is a mechanism-based model which has presented fairly good results [17,18]. Moreover, its modified form (MD-SF-PF) which has simulated the RO membrane characteristic has had high consistency with experimental data [17].

In this model, membrane is assumed to have cylindrical micro porous. Therefore, the profiles of velocity and concentration are functions of both radial (ρ) and axial directions (ζ). The interaction between solute and the wall of membranes is defined by the Sutherland type potential function, which varies in radial direction of the pore [17–19]. The Friction parameter describes the hydrodynamic drag of pore wall on the solute and is defined as the ratio of solute diffusivity in free solution to solute diffusivity inside a pore [17–19].

The brief explanation of MD-SF-PF model based on input parameters of ANN is as follows. These parameters include model parameters (θ_1, θ_2, τ/ε), membrane properties [R_W and X_{A1}, X_{A2} (friction constants between solute and/or solvent and membrane, respectively)], operational conditions, such as the average longitude concentration of solute in membrane (C), pressure (P), and temperature (T).

The two-dimensionless parameters which represent the radial ρ and axial ζ coordination directions are introduced as below [17–19]:

$$\rho = \frac{r}{R_W} \tag{2}$$

$$\xi = \frac{Z}{\tau} \tag{3}$$

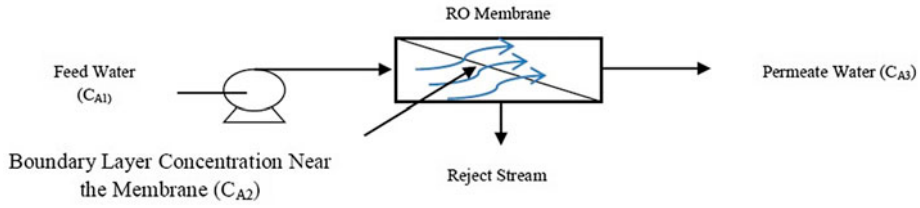

Fig. 1. Reverse osmosis membrane process.

where R_w is wall pore radius and τ is pore length. The differential equation expressing the velocity profile inside (α) the membrane pore was derived as the following:

$$\left[\frac{d^2\alpha(\rho)}{d\rho^2}+\frac{1}{\rho}\frac{d\alpha(\rho)}{d\rho}\right]+\frac{1}{\beta_1}\left[\frac{\Delta P}{\pi_2}-\frac{\pi_2\sigma_2(\rho)-\pi_3\sigma_3(\rho)}{\pi_2}\right] - \frac{1}{\beta_1}\left(1-\frac{1}{b(\rho)}\right)[\alpha(\rho)+\omega(\rho)]\left[1+\frac{1-(\frac{\pi_3}{\pi_2})k*(\rho)}{\exp[(\alpha(\rho)+\omega(\rho)]-1}\right] \times \exp(-\Phi(\rho,\ 0))=0 \tag{4}$$

where

$$\beta_1=\frac{\eta D_{AB}}{R_W^2\pi_2} \tag{5}$$

$$\sigma_2(\rho)=1-\exp(1-\Phi(\rho,\ 0)) \tag{6}$$

$$\sigma_3(\rho)=1-\exp(1-\Phi(\rho,\ 1)) \tag{7}$$

$$\omega(\rho)=\frac{V_A}{RT}[\Delta P-(\sigma_2(\rho)\pi_2-\sigma_3(\rho)\pi_3)] \tag{8}$$

$$k*(\rho)=\frac{\exp(-\Phi(\rho,\ 1))}{\exp(-\Phi(\rho,\ 0))} \tag{9}$$

$$\alpha(\rho)=\frac{U_B(\rho)\tau}{D_{AB}} \tag{10}$$

The osmotic pressure is obtained from Van't Hoff's equation:

$$\pi=(\upsilon^+ +\upsilon^-)C_ART \tag{11}$$

For the calculation of separation factor and fluxes in the mathematical modeling of membranes, the existence of concentration is inevitable and it is calculated from the concentration equation.

$$C_{A3}=C\left[1+CRT\frac{l_1}{l_3}\right]^{-1} \tag{12}$$

In which:

$$l_1=\int_0^1\alpha(\rho)\rho\,d\rho \tag{13}$$

$$l_3=\int_0^{1-\lambda}[\alpha(\rho)+\omega(\rho)]\left(\pi_2+\frac{\pi_2-k*(\rho)\pi_3}{\exp[(\alpha(\rho)+\omega(\rho)]-1}\right)\times\frac{\exp(-\Phi(\rho,0))}{b(\rho)}\rho\,d\rho$$

The solute and solvent fluxes are as below:

$$N_A=\varepsilon J_A=\frac{2}{X_{AB}}(\varepsilon/\tau)\int_0^{1-\lambda}\frac{[\alpha(\rho)+\omega(\rho)]}{b(\rho)} \times\left(\pi_2+\frac{\pi_2-k*(\rho)\pi_3}{\exp[(\alpha(\rho)+\omega(\rho)]-1}\right)\exp(-\Phi(\rho,\ 0))\rho\,d\rho \tag{14}$$

$$N_B=\varepsilon J_B=\frac{2}{X_{AB}}(\varepsilon/\tau)CRT\int_0^1\alpha(\rho)\rho\,d\rho \tag{15}$$

And the total flux is:

$$N_T=(N_A+N_B)=\frac{2}{X_{AB}}\left(\frac{\varepsilon}{\tau}\right)(l_3+CRT\,l_1) \tag{16}$$

And finally the pure solvent flux is:

$$N_P=A\Delta P,\quad A=\frac{CR_W^2}{8\eta(\tau/\varepsilon)} \tag{17}$$

A friction parameter b (ρ), which is the ratio of solute diffusivity in free solution to solute diffusivity inside a pore, is used to describe the hydrodynamic drag on the solute by the pore wall. This function described as below:

$$b=\frac{X_{AB}+X_{AM}}{X_{AB}}=\frac{D_{AB}}{D_{AM}} \tag{18}$$

$$b(\rho)=\begin{cases}b_{\text{Faxen}}\exp\left(\frac{E}{R_W(1-\rho)}\right) & \text{when } \rho<1-\lambda\\ \infty & \text{when } \rho\geq 1-\lambda\end{cases} \tag{19}$$

The solute–membrane interactions are expressed by a potential function, (Φ) which represents the net body force acting on the solute by the pore wall. In the "MD-SF-PF" model this function was considered as one dimensional.

$$\Phi(\rho,\zeta)=\begin{cases}\frac{\theta_1}{R_W}e^{\theta_2\rho^2} & \text{when } \rho<1-\lambda\\ \infty & \text{when } \rho\geq 1-\lambda\end{cases} \tag{20}$$

2.3. ANNs in general

One of the characteristics of ANNs which influences their performances is number of the layers. From this point of view, multilayer (ML) networks overcome single-layer networks for complex problems. It does not mean that increasing in number of layers, improve the performance of ANNs and many of them influence the MLP through over-fitting. The way that the neurons are connected to each other has a significant effect on the operation of ANNs. These connection ways are divided into two main types, feedforward and feedback. In a feedforward network, the information moves into only forward direction from the input layer through the hidden layer to the output layer. In the feedback network, the information moves from output to the input of hidden and finally to the input layers. The neuron sums up the weighted inputs and a bias and then passed it through a transfer function to produce the output for that neuron. A transfer function is a mathematical representation, in terms of spatial or temporal frequency, of the relationship between input and output which act on the sum of weighted inputs.

To show the performance and efficiency of the ANN, we need a way of evaluating its output error between the network and target output. Performance of the ANN is explained by different error functions such as MSE, RMSE, and correlation coefficient (R). The network is training to reduce the value of error functions between the ANN and the target output to increase its performances.

$$\mathrm{MSE} = \frac{\sum_1^n (P_m - P_e)^2}{n} \tag{21}$$

$$\mathrm{RMSE} = (\mathrm{MSE})^{\frac{1}{2}} \tag{22}$$

$$R = \frac{\sum_{i=1}^{Q}(P_{m,i} - P_{m,av})(P_{e,i} - P_{e,av})}{\sqrt{\sum_{i=1}^{Q}[(P_{m,i} - P_{m,av})^2 \sum_{i=1}^{Q}(P_{e,i} - P_{e,av})^2}} \tag{23}$$

where P_m is the target value, P_e is the network output, and n is the number of data-set.

2.4. Radial basic function

A RBF network (RBFN) was proposed by Broomhead and Lowe [34]. This network is a standard three layer feedforward neural network, i.e. the input layer, the nonlinear hidden layer (consists of Gaussian basic functions in this study), and a linear output layer. The major difference between RBFN and MLP network with error back propagation method exists in the hidden layer. A MLP neural network sums up the weighted input vectors but in a RBFN, the distance between input and center is used for learning process. Also, A RBFN is faster to learn and to use than a MLP.

The first layer of a RBFN consists of input data-set. For each neuron in hidden layer, the distance between the input data-set and the center is activated by a nonlinear radial basis function. This function is shown in the following equation:

$$\phi(x_i) = \exp\left[-(\parallel x_i - c_i \parallel b_1)^2\right] \tag{24}$$

where φ is the nonlinear RBF, x_i is the input vector, b_1 is bias in the hidden layer, and c_i is center vector.

Each hidden neuron receives all inputs (x_1, x_2, … , x_i) and produces one output. The value of each output, which has been produced by neurons in the hidden layer is between 0 and 1, depends on how close the input is to the center location. If the centers of neurons are closer to the inputs, they will have more contributions to the outputs. On the contrary, if neurons have centers away from inputs, then their outputs are invalidated and so vanished. Finally, the output layer neurons receive weighted inputs and RBFN output is given as follow equation:

$$y = \sum_{j=1}^{n} W_i \varphi(x_i) + b_2 \tag{25}$$

where y is RBFNN output, W_i connection weight which determines by the training process, b_2 bias in the output layer.

The RBFNNs have been used to apply on wide range of applications such as pattern classification, system identification, nonlinear function approximation, time-series prediction, and so on. A key point of RBFNN is determining the proper number of neurons in the hidden layer. If the number of neurons is too small, the output vector may be in low accuracy and too large numbers may cause overfitting of network. In a training process, the numbers of neurons in hidden layer is selected according to statistic properties of input data-set and then determine the centers and spread width for neurons. Various methods are proposed to choose the initial location of center, e.g. random selection, K-mean technique, max–min algorithms, etc. Spread width is an important parameter in the performance of RBFNNs. The value of spread width should be large enough to find the best

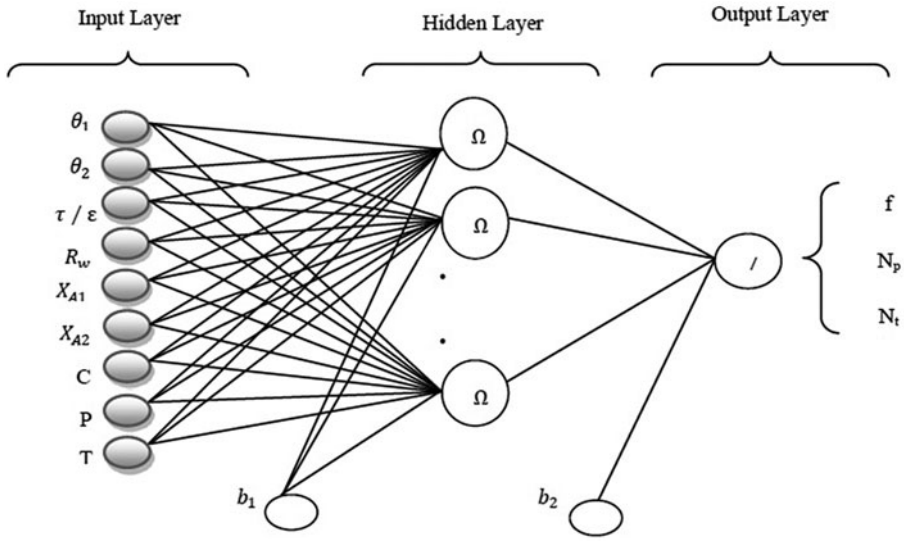

Fig. 2. Schematic representation of RBFNN employed in this study.

solution for a problem. Fig. 2 shows the structure and procedure work of RBFNN.

2.5. ANN inputs and outputs

The objective of MD-SF-PF model is to calculate separation characteristics: separation factor (f), pure solvent (N_p), and total flux (N_t). The connection between RO model and RBFNN is that the model parameters, membrane properties, and operational conditions were considered as input data of RBFNN. In this way, nine parameters are needed which are considered as inputs of the network. The input vector is consists of model parameters (θ_1, θ_2, τ/ε), membrane properties [R_W (pore radius), X_{A1}, X_{A2} (friction constants between solute and solvent and membrane respectively), and operational conditions such as the average longitude concentration of solute in membrane (C), pressure (P), and temperature (T).

A data-set consisting of 304 experimental data, which were gained by the four types of membranes, was applied in this regard. These experimental data were obtained by Mehdizadeh and Dickson [17]. Each data consist of nine-dimensional input vectors and three-dimensional output vectors. To observe the influence of inputs on each output, a one-dimensional output vector is used and the error functions were calculated for them separately.

3. Results and discussion

The entire data (304) were divided into two random parts: 80% as training data-set (243), and 20% as test data-set (61). For improving network application, training and test data-set have been distributed and normalized in (−1, 1) interval. The different values for spreading the width were tested and the optimum one was considered two.

Figs. 3–5 show the conformity of RBFNN training results and experimental data. Figs. 3–5 shows these results for separation factor, solute flux, and total flux, respectively.

From these figures, it was observed that a high conformity exists with experimental data and a minimum differences are visible in these data.

Figs. 6–8 show the MSE of outputs, i.e. separation factor (f), pure solvent flux (N_p), and total flux (N_t) vs. the number of neurons in hidden layer. These figures show a sharp drop in MSE when the number of neurons is less than 20. The proper number of neurons

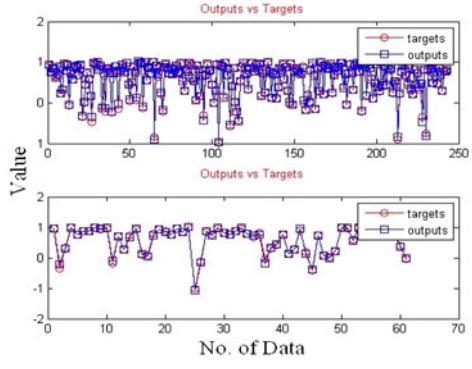

Fig. 3. The conformity of RBFNN training results with experimental data for separation factor.

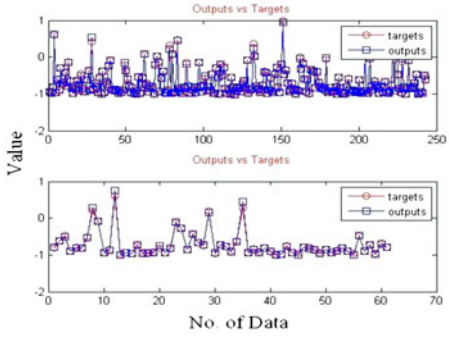

Fig. 4. The conformity of RBFNN training results with experimental data for solute flux.

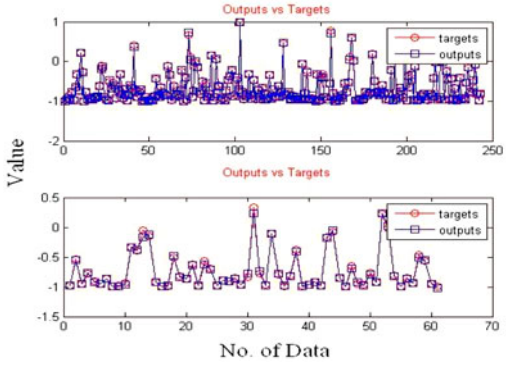

Fig. 5. The conformity of RBFNN training results with experimental data for total flux.

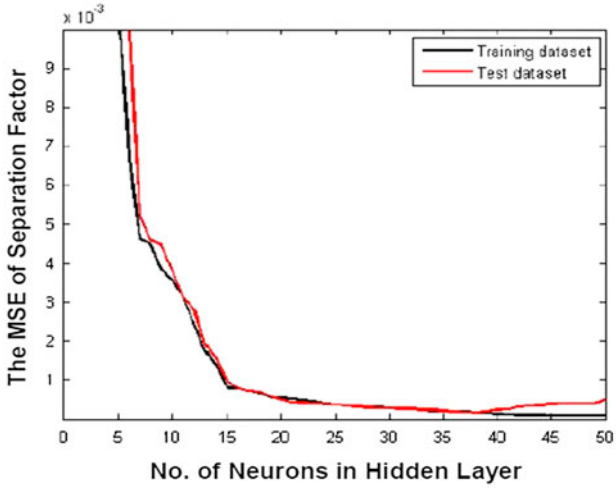

Fig. 6. MSE vs. the number of neurons in hidden layer for separation factor.

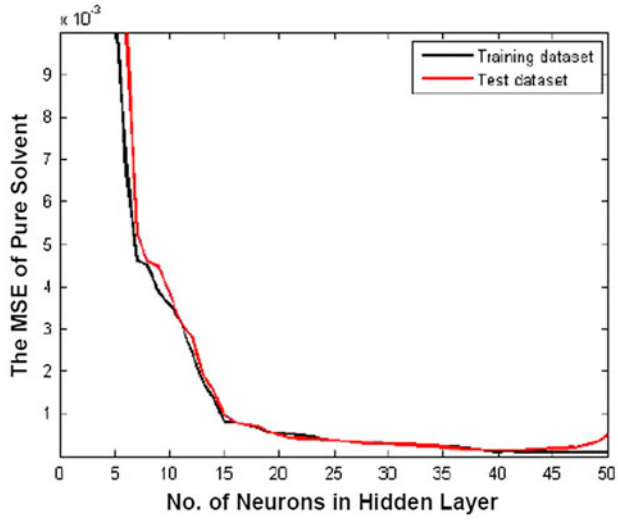

Fig. 7. MSE vs. the number of neurons in hidden layer for pure solvent flux.

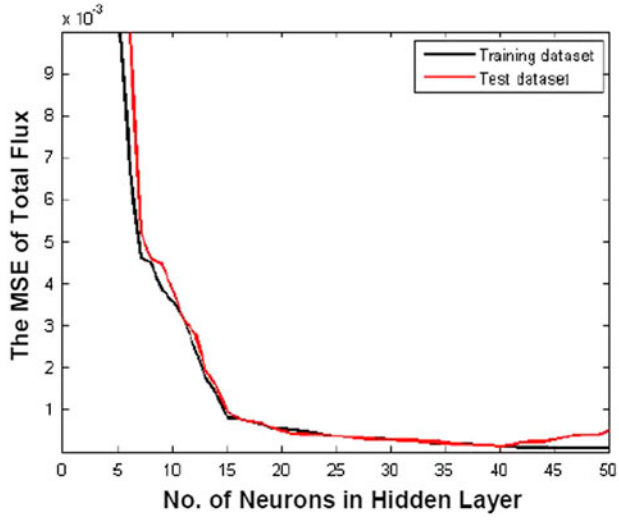

Fig. 8. MSE vs. the number of neurons in hidden layer for total flux.

should be selected to prevent over-fitting of network. As the figures illustrate, the MSE of training data-set decreased but the MSE of test data-set increased after maximum number of neurons reaches 38 for separation factor, 40 for pure solvent flux, and 41 for total flux. This means, if the number of neurons is more than the mentioned value, the network is facing over-fitting phenomena.

Figs. 9–11 explain target data vs. network output for three outputs which implemented with RBF neural network. As the figures show, correlation coefficient between the observed and predicted is as high as

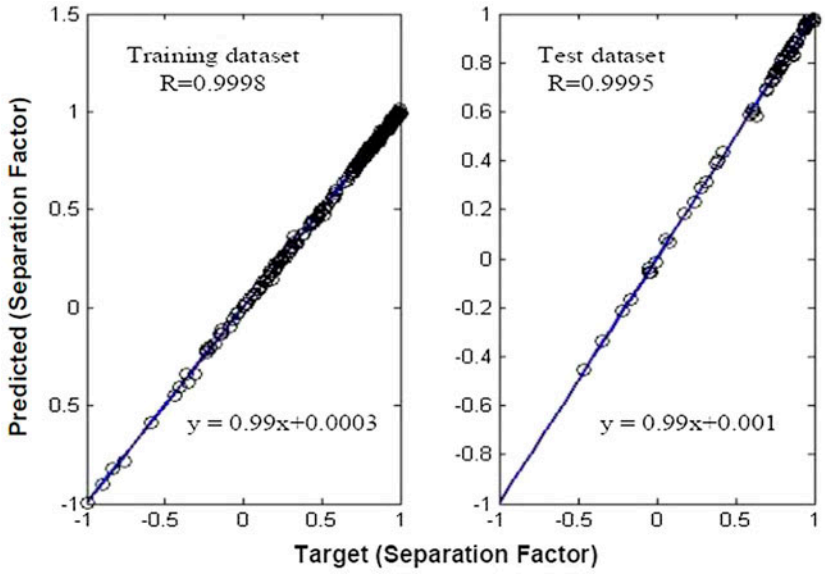

Fig. 9. Comparison RBFNN the predicted training and test data values vs. experimental data for separation factor.

0.9995 for separation factor, 0.9991 for pure solvent flux, and 0.9994 for total flux. All conditions such as slope and intercept are ideal for the results of RBFNN. All points of these figures were located near the $x = y$ line. This means that the target data and the predicted data have almost the same values.

After training process, the MSE for training and test data-set were obtained 0.00009 and 0.00016, respectively, for separation factor, 0.00013 and 0.00013 for pure solvent flux, 0.00009 and 0.00012 for total flux consequently. The simulation results show that RBFNN is an accurate method to predict performance of RO membranes. Table 1 shows the obtained results from trained network.

The comparison of results between RBFNN and BPNN (which was obtained by Moradi et al. [33])

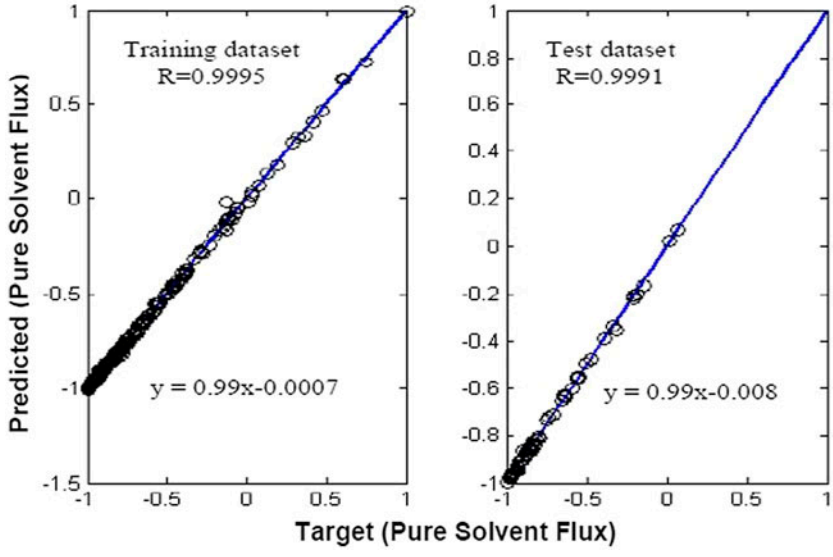

Fig. 10. Comparison RBFNN the predicted training and test data values vs. experimental data for pure solvent flux.

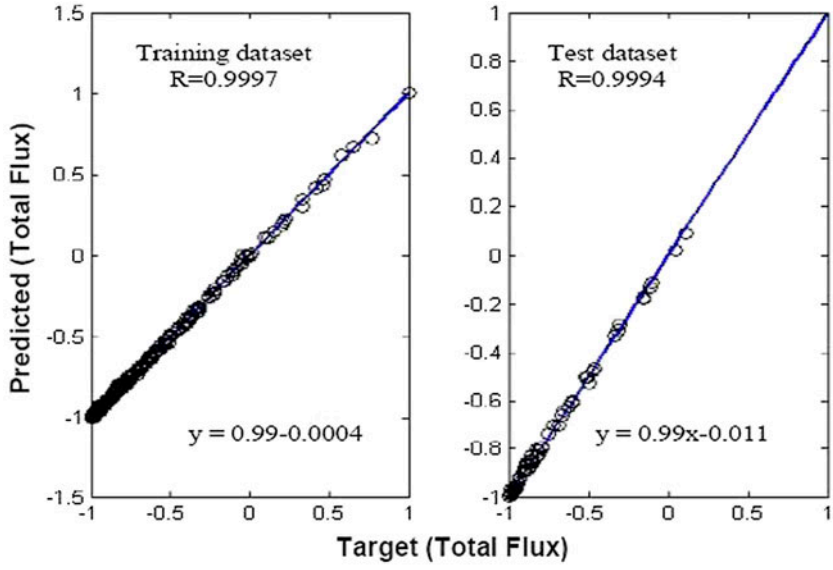

Fig. 11. Comparison RBFNN the predicted training and test data values vs. experimental data for total flux.

Table 1
Performance of RBFNN in prediction of RO membrane performances

RO performance	MSE	RMSE	*R*
Separation factor	0.00016	0.012	0.9995
Pure solvent flux	0.00013	0.011	0.9991
Total flux	0.00012	0.010	0.9994

show a clear superiority of our network compare to them. Finally, RBFNN can be used with high confidence to predict the performances of RO membranes in industrial applications by negligible error.

4. Conclusion

Due to complex and nonlinear equations of MD-SF-PF model, the necessity of a simple technique, which could have the capability of the predication of RO membrane performances, is inevitable. In the present study, a radial basic neural network RBFNN was developed to predict the performances of RO membranes. Implementation of the RBFNN lets to fast training of the network. The results confirm the advantage of RBFNN for the prediction of RO membranes performances identically. It is obvious that RBFNN can be used as an assured method to predict separation factor, pure solvent flux, and total flux with a high accuracy comparing to the numerical and other ANNs.

List of symbols

$b(\rho)$ — friction function, dimensionless
C — molar density of solution (kmol/m^3)
$C_A(r, Z)$ — concentration of solute inside a pore (kmol/m^3)
D_{AB} — solute diffusivity in free solution (m^2/sec)
D_{AM} — solute diffusivity inside the pore (m^2/sec)
f' — theoretical separation, dimensionless
$J_{A,r}(r)$ — radial component of solute flux through a single pore (kmol/m^2 s)
$J_{A,z}(r)$ — axial component of solute flux through a single pore (kmol/m^2 s)
l_1 and l_3 — definite integral, dimensionless
N_i — flux of i through membrane (kmol/m^2 s)
P — hydrostatic pressure (kPa)
r — cylindrical coordinate normal to the pore wall (m)
R — gas constant (kJ/kmol K)
T — temperature (K)
$U_i(r)$ — velocity of i inside the pore (m/s)
z — cylindrical coordinate parallel to the pore wall (m)
$k^*(\rho)$ — ratio of local partition coefficients at the ends of a pore for solute
OF — objective function
RMSD — parameter

Greek letters

$\alpha(\rho)$ — velocity defined, dimensionless
β_1 — parameter defined, dimensionless
ΔP — pressure drop across the membrane (kPa)
ε — fractional pore area of membrane, dimensionless

η — solution viscosity (kPa s)
θ_1 — potential parameter (m)
θ_2 — potential parameter, dimensionless
λ — parameter defined, dimensionless
ζ — axial coordinate, dimensionless
$\pi(r, Z)$ — osmotic pressure inside the pore (kPa)
π_i — osmotic pressure of solution at i (kPa)
ρ — radial coordinate, dimensionless
τ — average pore length taking tortuosity into account (m)
$\Phi(\rho, \zeta)$ — potential function dimensionless
$\sigma_2(\rho)$ — local Staverman (reflection) coefficient at feed–membrane interface
$\sigma_3(\rho)$ — local Staverman (reflection) coefficient at permeate–membrane interface
V_A — partial molar volume of solute (m^3/kmol)
$\omega(\rho)$ — parameter

Subscripts

A — solute
B — solvent
P — pure solvent (pure water)
M — membrane
T — total solution
W — pore wall
1 — feed solution
2 — feed at membrane interface
3 — permeate solution

References

[1] M.F. Abid, S.K. Al-Naseri, Q.F. Al-Sallehy, S.N. Abdulla, K.T. Rashid, Desalination of Iraqi surface water using nanofiltration membranes, Desalin. Water Treat. 29 (2011) 174–180.
[2] M. Mulder, Basic Principles of Membrane Technology, second ed., Kluwer Academic Publishers, Dordrecht, Boston, 1996.
[3] W.R. Baker, Membrane Technology and Applications, second ed., John Wiley & Sons Ltd, California, 2000.
[4] M. Soltanieh, W.N. Gill, Review of reverse osmosis membranes and transport models, Chem. Eng. Commun. 12 (1981) 279.
[5] O. Kedem, A. Katchalsky, Thermodynamic analysis of the permeability of biological membranes to non-electrolytes, Biochim. Biophys. Acta 27 (1958) 229–246.
[6] K.S. Spiegler, O. Kedem, Thermodynamics of hyperfiltration (reverse osmosis): Criteria for efficient membranes, Desalination 1 (1966) 311–326.
[7] H.K. Lonsdale, U. Merten, R.L. Riley, Transport properties of cellulose acetate osmotic membranes, J. Appl. Polym. Sci. 9 (1965) 1341–1362.
[8] G. Vakili-Nezhaad, Z. Akbari, Modification of the extended Spiegler–Kedem model for simulation of multiple solute systems in nanofiltration process, Desalin. Water Treat. 27 (2011) 189–196.
[9] T.K. Sherwood, P.L.T. Brian, R.E. Fisher, Desalination by reverse osmosis, I & EC Fund. 6 (1967) 2–12.
[10] H. Burghoff, K. Lee, W. Pusch, Characterization of transport across cellulose acetate membranes in the presence of strong solute–membrane interactions, J. Appl. Polym. Sci. 25 (1980) 323.
[11] S. Sourirajan, Reverse Osmosis, Academic Press, New York, NY, 1970.
[12] G. Jonsson, C.E. Boesen, Water and solute transport through cellulose acetate reverse osmosis membranes, Desalination 17 (1975) 145–165.
[13] S. Kimura, S. Sourirajan, Analysis of data in reverse osmosis with porous cellulose acetate membranes used, AIChE J. 13(3) (1967) 497–503.
[14] A.H. Hashim, Flow transport modelling of feed species (water and salt) through a seawater RO membrane, Desalin. Water Treat. 51 (2013) 1385–1404.
[15] T. Matsuura, Y. Taketani, S. Sourirrajan, Estimation of interfacial forces governing the reverse osmosis system: Nonionized polar organic solute-water-cellulose acetate membrane, in: A.F. Turbak (Ed.), Synthetic membranes, ACS Symposium, Series American Chemical Society, Washington, 1981 (Chapter 19).
[16] K.T. Chan, T. Matsuura, S. Sourirajan, Interfacial forces, average pore size and pore size distribution of ultrafiltration membranes, Ind. Eng. Chemi. Prod. Res. Dev. 21 (1982) 605–612.
[17] H. Mehdizadeh, J.M. Dickson, Theoretical modification of the surface force-pore flow model for reverse osmosis transport, J. Membr. Sci. 42 (1989) 119–145.
[18] H. Mehdizadeh, Modeling of Transport Phenomena in Reverse Osmosis Membranes, PhD thesis, McMaster University, Canada, 1990.
[19] A. Golnari, A. Moradi, A. Soltani, Effects of different potential functions on modeling of RO membrane performance by use of an advanced model, Res. Chem. Intermed. 39 (2013) 2603–2619.
[20] W.S. McCulloch, W. Pitts, A logical calculus of the ideas immanent in nervous activity, Bull. Math. Biophys. 5 (1943) 115–133.
[21] H. Niemi, A. Bulsari, S. Palosaari, Simulation of membrane separation by neural networks, J. Membr. Sci. 102 (1995) 185–191.
[22] H. Niemi, S. Palosaari, Calculation of permeate flux and rejection in simulation of ultrafiltration and reverse osmosis processes, J. Membr. Sci. 84 (1993) 123–137.
[23] N. Abbas, Al-Bastaki, Modeling of an RO water desalination unit using neural networks, Chem. Eng. J. 114 (2005) 139–143.
[24] H. Al-Zoubi, N. Hilal, N.A. Darwish, A.W. Mohammad, Rejection and modelling of sulphate and potassium salts by nanofiltration membranes: Neural network and Spiegler–Kedem model, Desalination 206 (2007) 42–60.
[25] Y. Zhao, J.S. Taylor, S. Chellam, Predicting RO/NF water quality by modified solution diffusion model and artificial neural networks, J. Membr. Sci. 263 (2005) 38–46.
[26] G.R. Shetty, S. Chellam, Predicting membrane fouling during municipal drinking water nanofiltration using artificial neural networks, J. Membr. Sci. 217 (2003) 69–86.
[27] Y.G. Lee, Y.S. Lee, J.J. Jeon, S. Lee, D.R. Yang, I.S. Kim, J.H. Kim, Artificial neural network model for optimizing operation of a seawater reverse osmosis desalination plant, Desalination 247 (2009) 180–189.

[28] D. Libotean, J. Giralt, F. Giralt, R. Rallo, T. Wolfe, Y. Cohen, Neural network approach for modeling the performance of reverse osmosis membrane desalting, J. Membr. Sci. 326 (2009) 408–419.
[29] M. Khayet, C. Cojocaru, M. Essalhi, Artificial neural network modeling and response surface methodology of desalination by reverse osmosis, J. Membr. Sci. 368 (2011) 202–214.
[30] M. Jafar, A. Zilouchian, Adaptive receptive fields for radial basis functions, Desalination 135 (2001) 83–91.
[31] H. Chen, A.S. Kim, Prediction of permeate flux decline in crossflow membrane filtration of colloidal suspension: A radial basis function neural network approach, Desalination 192 (2006) 415–428.
[32] M.S. Noghabi, S.M.A. Razavi, S.M. Mousavi, Prediction of permeate flux and ionic compounds rejection of sugar beet press water nanofiltration using artificial neural networks, Desalin. Water Treat. 44 (2012) 83–91.
[33] A. Moradi, V. Mojarradi, M. Sacheshmehpour, Prediction of RO membrane performances by use of artificial neural network and using the parameters of a complex mathematical model, Res. Chem. Intermed. 39 (2013) 3235–3249.
[34] D.S. Broomhead, D. Lowe, Multivariable function interpolation and adaptive networks, Complex Syst. 2 (1988) 321–335.